

Catalysis Science & Technology

Accepted Manuscript



This is an *Accepted Manuscript*, which has been through the Royal Society of Chemistry peer review process and has been accepted for publication.

Accepted Manuscripts are published online shortly after acceptance, before technical editing, formatting and proof reading. Using this free service, authors can make their results available to the community, in citable form, before we publish the edited article. We will replace this *Accepted Manuscript* with the edited and formatted *Advance Article* as soon as it is available.

You can find more information about *Accepted Manuscripts* in the [Information for Authors](#).

Please note that technical editing may introduce minor changes to the text and/or graphics, which may alter content. The journal's standard [Terms & Conditions](#) and the [Ethical guidelines](#) still apply. In no event shall the Royal Society of Chemistry be held responsible for any errors or omissions in this *Accepted Manuscript* or any consequences arising from the use of any information it contains.

ARTICLE

The cascade synthesis of α,β -unsaturated ketones via oxidative C–C coupling of ketones and primary alcohols over ceria catalyst

Cite this: DOI: 10.1039/x0xx00000x

Zhixin Zhang,^{a,b} Yehong Wang,^b Min Wang,^b Jianmin Lu,^b Chaofeng Zhang,^b Lihua Li,^b Jingyang Jiang,^a and Feng Wang^{*b}

Received 00th January 201x,
Accepted 00th January 201x

DOI: 10.1039/x0xx00000x

www.rsc.org/

We herein report the oxidative C–C coupling of ketones and primary alcohols to produce α,β -unsaturated ketones in the absence of base additives. This cascade synthetic reactions were conducted at 150 °C in 12 h using heterogeneous CeO₂ catalyst. The conversion of acetophenone reached 74% with 89% selectivity of chalcone. A correlation between CeO₂ crystal plane and catalytic performance is established as the catalytic activities decrease in the sequence of (110) > (111) > (100). The characterizations with Raman spectroscopy, CO₂-temperature programmed desorption (CO₂-TPD), and *in-situ* active-site-capping tests have shown that the unusual catalysis of CeO₂ catalyst is attributed to the coexistence of basic and redox active sites. These sites synergistically catalyze the oxidation of alcohol to aldehyde and the Aldol condensation to ketones. Moreover, the CeO₂ catalyst can be reused for several times after calcination to remove the surface-adsorbed substances.

Introduction

α,β -Unsaturated ketone is a class of important chemicals, which have numerous applications such as pesticides and food additives.^[1] They are traditionally prepared by the classical Aldol condensation reaction between ketones and aldehydes.^[2] The direct C–C bond coupling of ketones with primary alcohols is a more promising and economical process in synthesizing α,β -unsaturated ketones. The tandem reactions combine the oxidation (or dehydrogenation) of alcohols to aldehydes, and the Aldol condensation of aldehydes with ketones with minimal work-up and less waste production (e.g., efficiency in catalyst utilization, without isolation of aldehyde intermediates).^[3] The tandem reactions have been recently studied using bifunctional catalysts, which consist of precious metals with active sites for oxidative conversion, and alkaline supports with active sites for condensation reaction, such as the catalysts of Pd/AlO(OH),^[4] Pd/MgO–Al₂O₃,^[5] Pt/CeO₂,^[6] or Au/AlO(OH).^[7] But the majority of the reported processes still require alkali additives.^[8]

The development of inexpensive and highly efficient non-precious metal catalysts have drawn great attention in the α,β -unsaturated ketones synthesis, such as early-transition-metal nitrides (TiN, NbN, and NbCN).^[9] But the preparation of these materials involves the nitridation of the parent oxides under fierce conditions. Recently, Chen *et al.*^[10] used the metal oxide CrO₃ as a catalyst. However, the chromium species is dissolved

homogeneously in the reaction system and the use of chromium is environmental unfriendly. Therefore, it is desirable to develop an active, robust, and green catalyst for the cascade synthesis of ketones.

In general, the oxidative dehydrogenation of alcohols is a redox process and the Aldol condensation of aldehydes with ketones is catalyzed by acids or bases. Therefore, the expected catalyst for this tandem reaction is required to possess both redox sites and acid or base sites. CeO₂ has both redox and acid-base sites and has been widely used in various catalytic reactions, which have been well reviewed by Laurence Vivier and other researchers.^[11] We and other investigators have recently discovered that CeO₂ is a highly active and selective catalyst in the Prins condensation,^[12] transformylation,^[13] CO₂ fixation^[14] and other organic reactions^[15] because of its redox and acid-base properties.

Herein, we report that CeO₂ is an efficient catalyst for the cascade synthesis of α,β -unsaturated ketones from ketones and primary alcohols without base additive. Various ketones and primary alcohols were transformed to the corresponding α,β -unsaturated ketones over CeO₂. Besides, the catalyst is robust and can be reused several times with comparable results. Detailed studies have revealed that the performance of CeO₂ in tandem reactions is attributed to its unique catalytic properties.

Experimental

Materials

Chemicals and oxides were of analytical grade, purchased from Aladdin Chemicals, and used without further purification.

CeO₂ preparation

The CeO₂ sample was prepared by a conventional precipitation method.^[12] Briefly, 5.0 g of Ce(NO₃)₃·6H₂O was dissolved in 100 mL of Millipore-purified water (18 mΩ·cm), and the solution was adjusted to pH = 11.0 by the addition of NH₄OH (3.4 M) under magnetic stirring at room temperature. The resulting gel mixture was washed with pure water, dried in an oven at 120 °C for 12 h, and calcined at 500 °C in air (50 mL min⁻¹) for 4 h. To obtain CeO₂ of different morphologies, Ce(NO₃)₃·6H₂O was used as the cerium source. The preparation of different morphologies of CeO₂ samples was previously reported by our group and other groups.^[12-13, 16] Briefly, 0.868 g of Ce(NO₃)₃·6H₂O and an appropriate amount of NaOH (0.016–15 g) were dissolved in 5 mL and 35 mL of deionized water, respectively. Then, these two solutions were mixed in a Teflon bottle, and this mixture was stirred for 30 min at room temperature, and finally formed a milky slurry. Subsequently, the Teflon bottle with this mixture was held in a stainless steel vessel autoclave, which was then placed in an oven at temperatures in the range of 100–180 °C for 12 h or 24 h. After the hydrothermal treatment, the resulting precipitate was separated by centrifugation, thoroughly washed with deionized water and ethanol, followed by drying at 60 °C in air for 12 h.

Catalytic reactions and product analyses

In a typical reaction, the catalyst was added into a screw capped glass pressure vessel with a stirring bar. A solution of 58 μL acetophenone (0.5 mmol) and 78 μL benzyl alcohol (0.75 mmol) in 2 mL solvent was added, and the reactor was screwed tightly and heated to the set value in an oil bath. The products of the reaction were analyzed by gas chromatography (GC, Agilent 7890A) and gas chromatography-mass spectrometry (GC-MS) using an Agilent 7890A/5975C instrument equipped with an HP-5MS column (30 m in length, 0.25 mm in diameter). Authenticated samples were used to quantify the reactants and products. The calculation of conversion and selectivity is based on acetophenone.

CO₂ temperature-programmed desorption (CO₂-TPD)

The chemisorption of CO₂ on CeO₂ with different morphologies, fresh CeO₂, and used CeO₂ was conducted in a U-type quartz tube. In a typical CO₂-TPD experiment, 35 mg of dried sample was placed in the quartz tube and pretreated in flowing Ar at 210 °C for 1 h. Then, the sample was cooled to 30 °C and successive pulses of CO₂ were injected, using Ar (30 mL min⁻¹) as the carrier gas, until no change in the CO₂ concentration was detected. After CO₂ adsorption, the sample

was flushed with Ar (30 mL min⁻¹) for 10 min. The CO₂ desorption was carried out by increasing sample temperature from 30 to 600 °C (ramping rate: 10 °C min⁻¹) in an Ar gas flow (30 mL min⁻¹). The gas effluents during the CO₂ adsorption and desorption were analyzed by an on-line mass spectrometer (GSD320 Thermostar).

Catalyst characterizations

Powder X-ray diffraction (XRD) patterns were acquired using a PANalytical X-Pert diffractometer, applying Cu-Kα radiation at 40 kV and 40 mA. Continuous scans were collected over the 2θ range of 5° to 80°. Transmission electron microscopy (TEM) and high-resolution TEM (HRTEM) images were recorded on a JEOL-2100F electron microscope operating at 200 kV. Raman spectra were recorded on a micro-Raman spectrometer (Renishaw) equipped with a CCD detector using a He/Ne laser with a wavelength of 532 nm.

Results and discussion

Catalyst screen and reaction condition optimizations

In a preliminary experiment, the C–C coupling of acetophenone and benzyl alcohol was conducted over various solid oxides at 130 °C in 24 h (Table 1, entries 1–11). The reaction did not occur in the absence of catalyst (Table 1, entry 1). CeO₂ showed the highest activity with 64% acetophenone (**1**) conversion and 86% chalcone (**3**) selectivity (Table 1, entry 2). MgO, MnO₂, and Y₂O₃ gave 36%, 21%, and 18% acetophenone conversions, respectively (Table 1, entries 3–5). Other oxides, such as Nb₂O₅, Al₂O₃, V₂O₅, ZrO₂, SiO₂, and TiO₂ exhibited far lower activities (Table 1, entries 6–11).

Different solvents were examined in the synthesis of chalcone from acetophenone and benzyl alcohol (Table 1, entries 12–18). *p*-Xylene offered the highest conversion (74%) and the best chalcone selectivity (89%) at 150 °C in 12 h (Table 1, entry 12). Although 2-propanol gave the moderate conversion (49%), the chalcone selectivity was poor (8%) (Table 1, entry 13). Methanol and acetonitrile gave the low acetophenone conversions (~10%) and moderate chalcone selectivities (~65%) (Table 1, entries 14–15). In addition, the coupling reaction were much worse in dioxane, dimethyl formamide (DMF), and dimethyl sulfoxide (DMSO) (Table 1, entries 16–18). This is perhaps due to that these polar solvent molecules strongly adsorb on catalyst via coordination to coordinatively unsaturated metal ions (eg. (CH₃)₂-S=O→Ce³⁺, (CH₃)₂-N-C=O→Ce³⁺)^[17] and compete with polar substrates and reaction intermediates. In addition, these molecules would block the redox process of CeO₂. Reaction in Ar gas generated large amount of 1-phenylethanol (21% GC yield) and dihydrochalcone (15% GC yield) (Table 1, entry 19), which indicates this is a hydrogen-transfer reaction between acetophenone and benzyl alcohol. Oxygen is used to oxidize the active surface hydrogen species. Reaction in pure oxygen was detrimental to the conversion of acetophenone (Table 1, entry 20). This is perhaps due to the use of pure O₂ gas enhances the

oxidation rate of benzyl alcohol, benzaldehyde as the main oxidation product would accumulate and would be oxidized to benzoic acid, and benzoic acid would poison the basic sites of CeO₂.

The following optimization reactions focused on CeO₂ catalyst in order to achieve high yield of chalcone. Fig. 1 shows the catalytic results at temperatures of 40–150 °C. The conversion of acetophenone increased from 5% to 74% with the increase of temperature. Simultaneously, the selectivity of chalcone decreased from 100% to 89%. Dihydrochalcone (**4**) and 1-phenylethanol (**5**) as byproducts were generated at high temperature, indicating transfer hydrogenation reactions take place. Similar results have been obtained by several studies.^[8c, 8f, 8g]

Table 1 C–C coupling of acetophenone and benzyl alcohol over various oxides^a

<chem>Ph-C(=O)-CH3 + Ph-CH2-OH >>[catalyst] Ph-C(=O)-CH=CH-Ph + Ph-CH2-CH2-Ph + Ph-CH(OH)-CH3</chem>						
Entry	Catalyst	Solvent	Conv. (%) ^b	Sel. (%)		
				3	4	5
1	-	<i>p</i> -xylene	0	-	-	-
2	CeO ₂	<i>p</i> -xylene	64	86	5	8
3	MgO	<i>p</i> -xylene	36	90	-	10
4	MnO ₂	<i>p</i> -xylene	21	100	-	-
5	Y ₂ O ₃	<i>p</i> -xylene	18	45	-	55
6	Al ₂ O ₃	<i>p</i> -xylene	2	100	-	-
7	Nb ₂ O ₅	<i>p</i> -xylene	4	-	-	100
8	V ₂ O ₅	<i>p</i> -xylene	0	-	-	-
9	ZrO ₂	<i>p</i> -xylene	0	-	-	-
10	SiO ₂	<i>p</i> -xylene	0	-	-	-
11	TiO ₂	<i>p</i> -xylene	0	-	-	-
12 ^c	CeO ₂	<i>p</i> -xylene	74	89	5	6
13 ^d	CeO ₂	2-Propanol	49	8	-	92
14 ^d	CeO ₂	Methanol	11	67	-	33
15 ^d	CeO ₂	Acetonitrile	10	64	-	36
16 ^d	CeO ₂	Dioxane	8	-	-	100
17 ^d	CeO ₂	DMF	0	-	-	-
18 ^d	CeO ₂	DMSO	0	-	-	-
19 ^e	CeO ₂	<i>p</i> -xylene	64	45	23	32
20 ^f	CeO ₂	<i>p</i> -xylene	51	89	4	7

^a Reaction conditions: **1** (58 μL), **2** (78 μL), catalyst (100 mg), solvent (2 mL), 130 °C, 24 h, 1 atm air. ^b The conversion was based on acetophenone, determined by GC with the internal standard method. ^c 150 °C for 12 h, isolated: 44 %. ^d 150 °C for 12 h. ^e 150 °C for 6 h in Ar. ^f 150 °C for 6 h in oxygen.

Optimization of the reaction time was conducted at 150 °C. As can be seen from the Fig. 2, the chalcone selectivity was above 84% throughout the reaction. The acetophenone conversion rapidly increased to 73% after 6 h and leveled off at 74% after 12 h, probably due to the strong adsorption of organic species on CeO₂.^[18] CeO₂ behaves as a truly heterogeneous catalyst, as proved by the hot filtration test (Fig. 2). According to the

discussion above, 12 h at 150 °C in *p*-xylene under air were chosen as the suitable reaction conditions for further experiments.

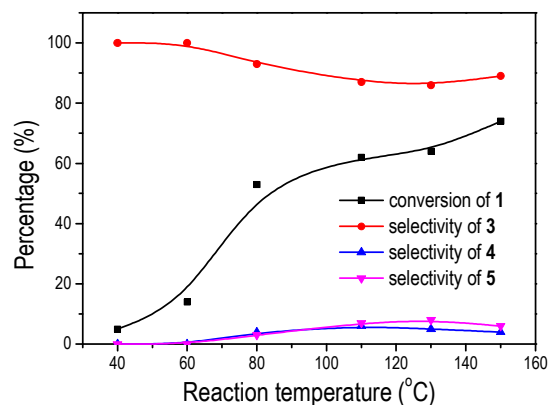


Fig. 1 Effect of reaction temperature on the catalytic performance of CeO₂ in the C–C coupling of acetophenone and benzyl alcohol. Reaction conditions: **1** (58 μL), **2** (78 μL), CeO₂ (100 mg), *p*-xylene (2 mL), 24 h, air.

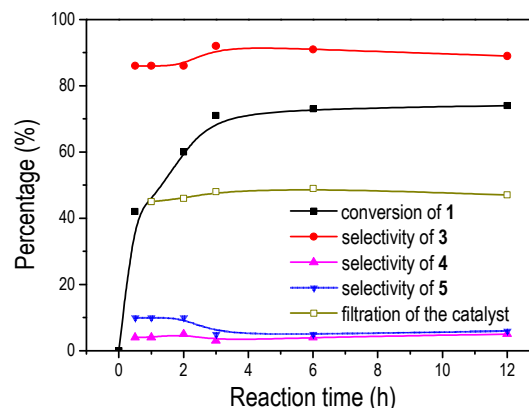


Fig. 2 Reaction profiles for the C–C coupling of acetophenone and benzyl alcohol over CeO₂. Reaction conditions: **1** (58 μL), **2** (78 μL), CeO₂ (100 mg), *p*-xylene (2 mL), 150 °C, air.

Coupling of various ketones and primary alcohols

In order to explore the substrate scope and functional group tolerance, we extended the CeO₂ catalyzed C–C coupling protocol to a wide range of ketones and primary alcohols (Table 2). We employed two different strategies to explore the efficiency of the CeO₂ for the synthesis of diverse α , β -unsaturated ketones. In the first strategy, various substituted benzyl alcohols were allowed to react with acetophenone. Substituted benzyl alcohols bearing an electron-donating or -withdrawing group reacted with acetophenone to afford the corresponding α , β -unsaturated ketones in moderate conversions (> 57%) and selectivities (> 64%) (**3a**, **3b**, **3c**). For

the *p*-nitrobenzyl alcohol, however, the desired coupling reaction is inhibited (**3d**) (11% acetophenone conversion), because the condensation of acetophenone with nitrobenzaldehyde is much more difficult than benzaldehyde (Supporting information, Table S1), which causes the accumulation of intermediates and seems to be detrimental to the coupling reaction. In the second strategy, the benzyl alcohol remained unchanged and was allowed to react with various ketones, such as *p*-substituted acetophenone, alkyl ketones, and cyclic ketones. The conversions of *p*-substituted acetophenone are in a medium level (> 55%) (**3e**, **3f**, **3g**) with the exception of *p*-nitroacetophenone (**3h**) (27% conversion). In the presence of *p*-nitroacetophenone, benzaldehyde yield was remarkably improved due to the oxidation of benzyl alcohol. When acetone was used as a substrate, the conversion of acetone reached 76% (**3i**) and dibenzylideneacetone was produced as the byproduct. For other alkyl ketones and cyclic ketones, such as 2-heptanone, cyclohexanone, and 1-tetralone, the desired products were obtained but in low conversions (23% ~31%) (**3j**, **3k**, **3l**).

Table 2 Scope of the coupling reaction of ketones with alcohols catalyzed by CeO₂^a

$\text{R}_1\text{C(=O)CH}_3 + \text{R}_2\text{CH}_2\text{OH} \xrightarrow[150\text{ }^\circ\text{C, 12 h, Air}]{\text{CeO}_2} \text{R}_1\text{C(=O)CH=CHR}_2$		
<p>3a conv. / sel.: 68% / 81% (IY 33%)^b</p>	<p>3b 57% / 79%</p>	<p>3c 66% / 64%</p>
<p>3d 11% / 100%</p>	<p>3e 55% / 87%</p>	<p>3f 55% / 88%</p>
<p>3g 69% / 77%</p>	<p>3h 27% / 58%</p>	<p>3i 76% / 84%</p>
<p>3j 31% / 88%</p>	<p>3k 27% / 100%</p>	<p>3l 23% / 80%</p>

^a Reaction conditions: **1** (0.5 mmol), **2** (0.75 mmol), CeO₂ (100 mg), *p*-xylene (2 mL), 150 °C, in 12 h, air. The conversions based on ketones consumption were determined by GC-MS. ^b Yield of isolated product.

Catalyst Stability

The recyclability of the CeO₂ catalyst was investigated. After reaction, spent CeO₂ was recovered by centrifugation, washed with ethanol, dried, and then used for a subsequent cycle. As depicted in Fig. 3, the fresh catalyst reached 66% yield of chalcone. However, deactivation of the catalyst (21% yield), with a color change from pale yellow to grey yellow, was observed in the first reuse. The possible reason of catalyst deactivation is that the reaction intermediate species blocks active sites on the catalyst surface. Accordingly, TPO-MS analysis indicates the obvious peaks of CO_x (*x* = 1, 2) appearing at around 255 °C (Figure S1). This test suggests that the

reaction intermediate adsorbed on CeO₂ surface can be removed by calcination. Therefore, before any successive use, the catalyst is calcined at 300 °C to remove the adsorbed organic species. The calcined CeO₂ can be reused for several times (Fig. 3). Although the catalytic activity of CeO₂ gradually decreased slightly during such repeated uses. The possible reason is that the specific area of the CeO₂ gradually decreased slightly during repeated calcination processes. These results indicate CeO₂ is a robust heterogeneous catalyst for this reaction.

Effects of the CeO₂ crystal planes

The relationship between the catalytic activity and the morphology (rod, octahedron, and cube)/crystal planes of nanostructured CeO₂ was investigated by performing the C–C coupling reaction. CeO₂ samples with different morphologies were synthesized according to procedures previously reported in the literature.^[12–13, 16] The X-ray diffraction (XRD) patterns (Fig. S2) confirm the formation of ceria based on the diffraction peaks observed at $2\theta = 28.7^\circ, 33.2^\circ, 47.7^\circ$ and 56.6° (JCPDS 65-2975), corresponding to the (111), (200), (220) and (311) planes of a CeO₂ fluorite-type structure, respectively, with no significant impurities observed. According to high-resolution transmission electron microscope (HRTEM) images (Fig. S3), these samples have different exposed crystal plane: (110) and (100) for rods, (111) for octahedra, and (100) for cubes. This result is in good agreement with Yan et al.^[19] The chalcone yield over the rod sample is 48% (Table 3, entry 1), whereas the octahedron sample and the cube sample only had 6% and 2% chalcone yield, respectively (Table 3, entries 2–3). In consideration of the BET surface area of CeO₂, the generation rate of chalcone per added surface area per hour (yield) was also calculated and compared. It can be found that the generation rate of chalcone over the rod sample is $3.953\text{ }\mu\text{mol m}^{-2}\text{ h}^{-1}$, which is about 3-fold and 4-fold of octahedron ($1.190\text{ }\mu\text{mol m}^{-2}\text{ h}^{-1}$) and cube ($0.926\text{ }\mu\text{mol m}^{-2}\text{ h}^{-1}$), respectively. The sequence of catalytic activity (rod > octahedron > cube) and the HRTEM result indicated that the (110) crystal plane of CeO₂ nanorods is the most active one for this reaction in these crystal planes.

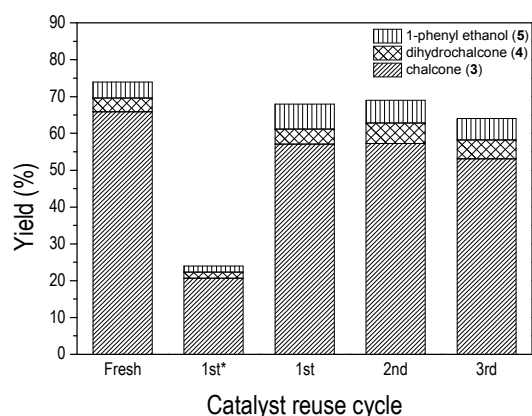


Fig. 3 Catalyst recycling for the C–C coupling of acetophenone and benzyl alcohol over CeO₂. Reaction conditions: **1** (58 μ L), **2** (78 μ L), CeO₂ (100 mg), catalyst (100 mg), *p*-xylene (2 mL), 150 $^{\circ}$ C, 12 h, air. 1st* was the first run of CeO₂ without calcination. 1st was the first run after calcination.

The formation energy of surface oxygen vacancy is a key parameter for the oxidation reactions.^[20] DFT theoretical studies indicate that the formation energies of ceria surface oxygen vacancies in the (110) surface are the lowest, followed by (100) and (111),^[21] which is in agreement with the results that the (110) plane exhibited the highest activity. In addition, the concentration of surface oxygen vacancy was also determined by Raman spectroscopy in the present study (Fig. S4). Two bands were observed in these three samples, which were ascribed to the Raman-active F_{2g} vibrational mode of the CeO₂ fluorite-type structure (the intense band at 462 cm⁻¹)^[22] and surface oxygen vacancy sites (the weak band at 590 cm⁻¹),^[23] respectively. The ratio of the integrated peak areas under the bands at 590 cm⁻¹ and 462 cm⁻¹ (A_{590}/A_{462}) can be used to quantify the relative concentration of surface oxygen vacancy sites.^[24] The calculated values were listed in the Table 4. The tendency of the A_{590}/A_{462} ratio matches well with the catalytic performance of these CeO₂ samples.

Table 3 C–C coupling of acetophenone and benzyl alcohol over different crystal planes of the CeO₂ catalyst^a

Entry	Morphology	Crystal plane	S (m ² g ⁻¹) ^b	Chalcone yield. (%) ^c
1	rod	(110)/(100)=2/1	86	48 (3.953) ^d
2	octahedron	(111)	21	6 (1.190)
3	cube	(100)	9	2 (0.926)

^a Reaction conditions: **1** (58 μ L), **2** (78 μ L), CeO₂ (100 mg), *p*-xylene (2 mL), 150 $^{\circ}$ C, for 12 h, under air. ^b S = BET surface area. ^c Yield = conversion \times selectivity, the conversions based on acetophenone consumption were determined by GC. ^d Data in parenthesis indicated the molar product per reaction time (h) per added surface area of CeO₂ (unit: μ mol m⁻² h⁻¹).

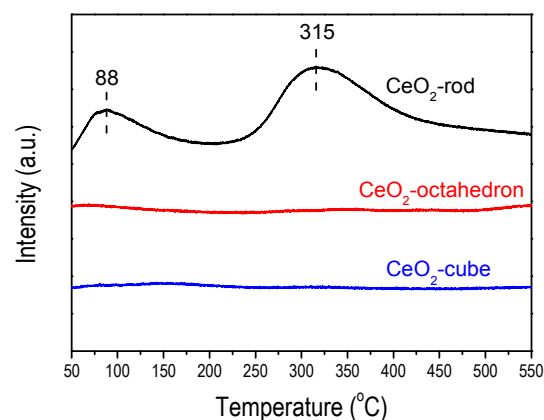


Fig. 4 CO₂-TPD profiles of the CeO₂ with different morphology.

Furthermore, the effect of crystal plane on the basic properties of the CeO₂ catalysts was investigated by the CO₂-TPD technique. The CO₂-TPD peaks representing the base strength distribution of CeO₂ catalysts with different morphologies are presented in Fig. 6. In general, the numbers of weak, medium, and strong catalyst basic sites are estimated from the CO₂ desorption peak area under their TPD curves for the temperature range of 100 \sim 250, 250 \sim 400, and >400 $^{\circ}$ C.^[25] According to Fig. 6, the CO₂-TPD profile for CeO₂-rod showed two peaks centred around 88 $^{\circ}$ C and 315 $^{\circ}$ C, which were attributed to the weak and medium basic sites, respectively. However, there was no obvious CO₂ desorption peak for the CeO₂-octahedron and CeO₂-cube samples in the range of 50–550 $^{\circ}$ C. In detail, the distribution of the number of basic sites for the CeO₂ catalysts are listed in Table 4. As revealed in Fig. 6 and Table 4, the different distribution of basic sites for each catalyst indicates that the basicity and base strength distribution are influenced by the morphology of the CeO₂ catalysts and the (110) places shows a large number of weak and medium basic sites as compared to the (111) and (100) places.

Table 4 Concentration of oxygen vacancy and basic sites of CeO₂ with different morphology

Entry	Catalyst	A_{595}/A_{462} ^a	Basic sites (μ mol/g) ^b		
			weak	medium	total
1	CeO ₂ -rod	0.077	659	680	1339
2	CeO ₂ -octahedron	0.003	0	0	0
3	CeO ₂ -cube	0.001	0	0	0

^a A_{595}/A_{462} means intrinsic oxygen vacancy concentration of CeO₂ samples based on Raman spectroscopy. ^b Determined by CO₂-TPD expressed in micromoles CO₂ desorbed per gram catalyst.

To sum up, the (110) crystal plane is considered as the most active plane of CeO₂ due to its substantial enhanced redox and basic properties.

Table 5 Effect of capping agent on the catalytic performance of CeO₂ in the C-C coupling of acetophenone with benzyl alcohol.^a

Entry	Capping agent (0.58 mmol)	Conv. (%) ^b	Sel. (%)		
			3	4	5
1	-	39(43) ^c	96	2	2
2	Pyridine	37(31) ^c	99	-	1
3	Benzoic acid	0(11) ^c	-	-	-

^a Reaction conditions: **1** (58 μ L), **2** (78 μ L), CeO₂ (100 mg), *p*-xylene (2 mL), 100 °C, for 12 h, under Air. ^b The conversions based on acetophenone consumption were determined by GC-GS. ^c Date in parenthesis indicated the conversion of benzyl alcohol.

In situ capping tests

In order to make clear the influence of the surface acid-base properties of CeO₂ for the coupling reaction, the in-situ acid-base sites capping experiments have been performed. Usually, pyridine strongly reacts with the acidic sites of the catalyst,^[26] while benzoic acid poisons the basic sites.^[27] In the present work, the C-C coupling of acetophenone and benzyl alcohol was performed in the presence of pyridine or benzoic acid. The conversion was almost the same with or without the addition of pyridine. (37% in Table 5, entry 2 vs. 39% in Table 5, entry 1). In contrast, the addition of benzoic acid completely suppressed the reaction (Table 5, entry 3). These results indicate that the basic sites of CeO₂ are the catalytically active center for the reaction. Otherwise, the conversions based on the benzyl alcohol consumption were also showed in the column of conversion (Table 5). In the presence of benzoic acid (0.58 mmol), the aerobic oxidation of benzyl alcohol was constrained.

Reaction mechanism

In this study, CeO₂ acted as bifunctional catalyst and played two roles: oxidative dehydrogenation of alcohol and Aldol condensation of benzaldehyde with acetophenone. In the first step, although the alcohol is oxidized by lattice oxygen, the CeO₂ acts as catalyst. Because if the benzyl alcohol oxidation was conducted in the absence of oxygen, the conversion of benzyl alcohol was below 1 %. In addition, the recycling of CeO₂ without calcination in the benzyl alcohol oxidation also proved this point (See Table 6). Fresh CeO₂ gave 22 % benzyl alcohol conversion (Table 6, Entry 1). After reaction, used CeO₂ was recovered by centrifugation, washed with ethanol, dried, and then used for a subsequent cycle. As depicted in Table 6, Entry 2, the used CeO₂ obtained 29% benzyl alcohol conversion. It can be concluded that CeO₂ worked as catalyst. Moreover, it is generally accepted that benzyl alcohol oxidation over ceria proceeds via Mars-van Krevelen mechanism.^[28] Tamura et al have also reported that CeO₂ acts as a reusable and efficient heterogeneous catalyst for the imine formation from benzyl alcohol and aniline.^[15a] In the first step of this reaction, oxidative dehydrogenation of benzyl alcohol with oxygen

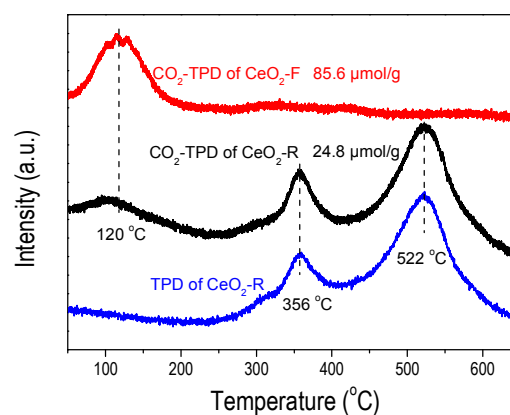
species occurs on the redox sites of CeO₂ catalyst. Benzyl alcohol removes the lattice oxygen, leading to the formation of oxygen vacancy, then the oxygen vacancy is replenished with molecular oxygen through oxygen mobility.

Table 6 Benzyl alcohol oxidation over CeO₂^a

Entry	Catalyst	Conv. (%) ^b	Sel. (%)	
			6	7
1	Fresh CeO ₂	22	92	8
2	Used CeO ₂ ^c	29	92	8

^a Reaction conditions: **2** (0.5 mmol), Catalyst (100 mg), *p*-xylene (2 mL), 150 °C, for 5 h, 1 atm air. ^b The conversions and selectivity based on benzyl alcohol consumption were determined by GC. ^c The used CeO₂ was recovered by centrifugation, washed with ethanol for three times, and dried at 100 °C.

For the Aldol condensation of acetophenone with benzaldehyde over basic sites of CeO₂, the organic species produced by benzaldehyde oxidation would blocks basic sites on the basic sites. CO₂-TPD of used CeO₂ (CeO₂-R) and fresh CeO₂ (CeO₂-F) (See Fig. 5) proved this point. In addition, the deposited organic species desorption were confirmed by comparison between TPD of CeO₂-R and CO₂-TPD of CeO₂-R. As depicted in Fig. 5, the peaks around 356 and 522 °C were attributed to the organic species desorption. The concentration of basic sites for the CeO₂-F and CeO₂-R were calculated based on the desorption peak of CO₂ around 120 °C, and the values were 85.6 μ mol/g and 24.8 μ mol/g, respectively. We think the concentration difference (60.8 μ mol/g) between this two values could reflect the amount of deposited organic species. Calcination is a common manner of catalyst regeneration. The organic species which blocks basic sites on the catalyst surface would be removed by calcination and the catalyst would be recovered. Thus, we suppose that the C-C coupling reaction was a catalytic reaction over CeO₂.

**Fig. 5** CO₂-TPD of CeO₂-F and CeO₂-R and TPD of CeO₂-R

Kinetic analysis of the alcohol oxidation and Aldol reaction over CeO_2 catalyst were carried out at 150 °C. The initial concentrations of benzyl alcohol and acetophenone were 0.36 mol/L and 0.23 mol/L, respectively. The reaction rate values are based on data from Fig. 6. and are calculated to be $2.48 \times 10^{-4} \text{ mol L}^{-1} \text{ min}^{-1}$ and $9.79 \times 10^{-5} \text{ mol L}^{-1} \text{ min}^{-1}$, respectively. Thus, it can be concluded that the Aldol condensation is a slower step and could be the rate determining step.

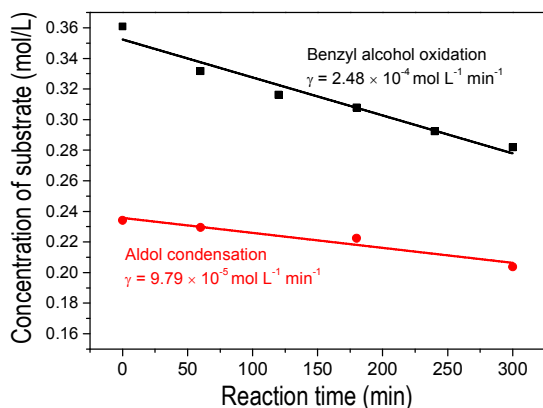
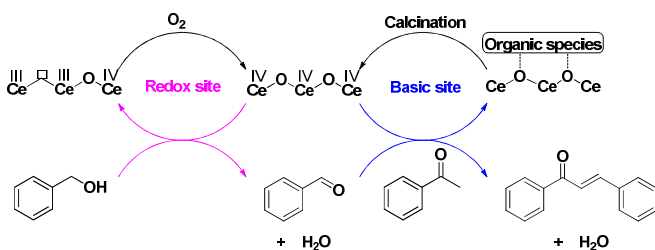


Fig. 6 The kinetic analysis of the oxidation of benzyl alcohol and the Aldol condensation of acetophenone with benzaldehyde.

Reaction conditions: 1) Benzyl alcohol oxidation: benzyl alcohol 0.75 mmol, *p*-xylene 2 mL, CeO_2 100 mg, 150 °C, 1 atm Air; 2) Aldol condensation: acetophenone 0.5 mmol, benzaldehyde 0.75 mmol, *p*-xylene 2 mL, CeO_2 100 mg, 150 °C, Ar.

On the basis of the results above, a reaction mechanism for the C–C coupling of acetophenone and benzyl alcohol over CeO_2 catalyst can be proposed as in Scheme 1. First, the formation of benzaldehyde by the oxidative dehydrogenation of benzyl alcohol with oxygen species occurs on the redox sites of CeO_2 and Ce will be reduced from tetravalent (+4) to trivalent (+3). Then, the obtained benzaldehyde reacts with acetophenone to afford the chalcone over the basic sites of CeO_2 . At last, the target product chalcone desorbs and the active site is regenerated by calcination to remove the chemisorbed organic species for next cycle. This possible reaction mechanism is similar to the mechanism of imine formation from benzyl alcohol and imine over CeO_2 reported by Tamura.^[15a]



Scheme 1. Tentative reaction mechanisms for the C–C coupling of acetophenone and benzyl alcohol over CeO_2 .

Conclusions

In summary, we have reported an efficient C–C coupling of ketones and primary alcohols to produce α,β -unsaturated ketones over CeO_2 catalyst in the absence of alkaline additives. Strong crystal plane effects of CeO_2 on the C–C coupling reaction have been identified. The (110) plane of CeO_2 nanorods is the most active plane for the reaction among the three low index planes (110), (111), and (100). Raman spectra and CO_2 -TPD characterizations have suggested that the catalytically active sites of CeO_2 consist of surface redox and base sites. The reaction involves the oxidation dehydrogenation of benzyl alcohol on the redox sites and the Aldol condensation of benzaldehyde and acetophenone on the base sites. This study will be helpful for the understanding of catalytic reactions over ceria catalyst.

Acknowledgements

This work was supported by the National Natural Science Foundation of China (21303189, 21422308) and Dalian Excellent Youth Foundation (2014J11JH126).

Notes and references

^a State Key Laboratory of Fine Chemicals, College of Chemistry, Faculty of Chemical Environmental and Biological Science and Technology, Dalian University of Technology, Dalian 116024, Liaoning, China.

^b State key Laboratory of Catalysis, Dalian National Laboratory for Clean Energy, Dalian Institute of Chemical Physics, Chinese Academy of Sciences, Dalian 116023, Liaoning, China.

*Corresponding author. Tel: +86-411-84379762; Fax: +86-411-84379762; E-mail: wangfeng@dicp.ac.cn

Electronic Supplementary Information (ESI) available: [details of any supplementary information available should be included here]. See DOI:10.1039/b000000x/

- (a) S. Nasir Abbas Bukhari, M. Jasamai and I. Jantan, *Mini-Rev. Med. Chem.* 2012, **12**, 1394; (b) Y. T. Liu, X. M. Sun, D. W. Yin and F. Yuan, *Res. Chem. Intermed.* 2013, **39**, 1037.
- M. J. Climent, A. Corma, S. Iborra and A. Velty, *J. Catal.* 2004, **221**, 474.
- (a) S. Sithambaram, R. Kumar, Y. Son and S. Suib, *J. Catal.* 2008, **253**, 269; (b) H. Sun, F. Z. Su, J. Ni, Y. Cao, H. Y. He and K. N. Fan, *Angew. Chem. Int. Ed.* 2009, **48**, 4390; (c) S. Sithambaram, Y. Ding, W. Li, X. Shen, F. Gaenzler and S. L. Suib, *Green Chem.* 2008, **10**, 1029; (d) A. Zanardi, J. A. Mata and E. Peris, *Chem. Eur. J.* 2010, **16**, 10502; (e) V. Cadierno, P. Crochet, J. Francos, S. E. Garcia-Garrido, J. Gimeno and N. Nebra, *Green Chem.* 2009, **11**, 1992.
- M. S. Kwon, N. Kim, S. H. Seo, I. S. Park, R. K. Cheedra and J. Park, *Angew. Chem.* 2005, **117**, 7073.

- 5 S. K. Jana, Y. Kubota and T. Tatsumi, *Stud. Surf. Sci. Catal.* 2007, **701**.
- 6 C. Chaudhari, S. M. A. H. Siddiki, K. Kon, A. Tomita, Y. Tai and K.-i. Shimizu, *Catal. Sci. Technol.* 2014, **4**, 1064.
- 7 S. Kim, S. W. Bae, J. S. Lee and J. Park, *Tetrahedron* 2009, **65**, 1461.
- 8 (a) G. Guillena, D. J. Ramón and M. Yus, *Angew. Chem. Int. Ed.* 2007, **46**, 2358; (b) T. D. Nixon, M. K. Whittlesey and J. M. J. Williams, *Dalton Trans.* 2009, 753; (c) B. W. J. Chen, L. L. Chng, J. Yang, Y. Wei, J. Yang and J. Y. Ying, *ChemCatChem* 2013, **5**, 277; (d) R. Martínez, G. J. Brand, D. J. Ramón and M. Yus, *Tetrahedron Lett.* 2005, **46**, 3683; (e) C. S. Cho, B. T. Kim, T. J. Kim and S. Chul Shim, *Tetrahedron Lett.* 2002, **43**, 7987; (f) R. Martínez, D. J. Ramón and M. Yus, *Tetrahedron* 2006, **62**, 8988; (g) C. S. Cho, B. T. Kim, T. J. Kim and S. C. Shim, *J. Org. Chem.* 2001, **66**, 9020; (h) T. Kuwahara, T. Fukuyama and I. Ryu, *Org. Lett.* 2012, **14**, 4703; (i) C. S. Cho, *J. Mol. Catal. A: Chem.* 2007, **267**, 49; (j) P. Satyanarayana, G. M. Reddy, H. Maheswaran and M. L. Kantam, *Adv. Synth. Catal.* 2013, **355**, 1859; (k) L. K. M. Chan, D. L. Poole, D. Shen, M. P. Healy and T. J. Donohoe, *Angew. Chem. Int. Ed.* 2014, **53**, 761; (l) M. L. Buil, M. A. Esteruelas, J. Herrero, S. Izquierdo, I. M. Pastor and M. Yus, *ACS Catal.* 2013, **3**, 2072; (m) S. Bhat and V. Sridharan, *Chem. Commun.* 2012, **48**, 4701; (n) C. Xu, X. M. Dong, Z. Q. Wang, X. Q. Hao, Z. Li, L. M. Duan, B. M. Ji and M. P. Song, *J. Organomet. Chem.* 2012, **700**, 214; (o) K. Taguchi, H. Nakagawa, T. Hirabayashi, S. Sakaguchi and Y. Ishii, *J. Am. Chem. Soc.* 2004, **126**, 72; (p) X. Cui, Y. Zhang, F. Shi and Y. Deng, *Chem. Eur. J.* 2011, **17**, 1021; (q) Y. M. A. Yamada and Y. Uozumi, *Org. Lett.* 2006, **8**, 1375; (r) G. Xu, Q. Li, J. Feng, Q. Liu, Z. Zhang, X. Wang, X. Zhang and X. Mu, *ChemSusChem* 2014, **7**, 105; (s) C. Cho, *J. Mol. Catal. A: Chem.* 2005, **240**, 55; (t) J. S. Jang, M. S. Kwon, H. G. Kim, J. W. Park and J. S. Lee, *Bull. Korean Chem. Soc.* 2012, **33**, 1617; (u) Y. M. A. Yamada and Y. Uozumi, *Tetrahedron* 2007, **63**, 8492.
- 9 (a) W. Yao, P. Makowski, C. Giordano and F. Goettmann, *Chem. Eur. J.* 2009, **15**, 11999; (b) A. Fischer, P. Makowski, J. O. Müller, M. Antonietti, A. Thomas and F. Goettmann, *ChemSusChem* 2008, **1**, 444.
- 10 Y. Li and D. Chen, *Chin. J. Chem.* 2011, **29**, 2086.
- 11 (a) J. Beckers and G. Rothenberg, *Green Chem.* 2010, **12**, 939; (b) L. Vivier and D. Duprez, *ChemSusChem* 2010, **3**, 654; (c) A. Trovarelli, *Catal. Rev. - Sci. Eng.* 1996, **38**, 439; (d) J. Kaspar, P. Fornasiero and M. Graziani, *Catal. Today* 1999, **50**, 285; (e) R. I. Walton, *Prog. Cryst. Growth Charact. Mater.* 2011, **57**, 93.
- 12 Y. Wang, F. Wang, Q. Song, Q. Xin, S. Xu and J. Xu, *J. Am. Chem. Soc.* 2012, **135**, 1506.
- 13 Y. Wang, F. Wang, C. Zhang, J. Zhang, M. Li and J. Xu, *Chem. Commun.* 2014, **50**, 2438.
- 14 R. Juárez, P. Concepcion, A. Corma and H. Garcia, *Chem. Commun.* 2010, **46**, 4181.
- 15 (a) M. Tamura and K. Tomishige, *Angew. Chem. Int. Ed.* 2015, **54**, 864; (b) M. Tamura, S. Siddiki and K. Shimizu, *Green Chem.* 2013, **15**, 1641; (c) M. Tamura, K. Noro, M. Honda, Y. Nakagawa and K. Tomishige, *Green Chem.* 2013, **15**, 1567; (d) M. Honda, S. Sonehara, H. Yasuda, Y. Nakagawa and K. Tomishige, *Green Chem.* 2011, **13**, 3406; (e) M. Tamura, T. Tonomura, K.-i. Shimizu and A. Satsuma, *Green Chem.* 2012, **14**, 717; (f) M. Tamura, T. Tonomura, K. Shimizu and A. Satsuma, *Green Chem.* 2012, **14**, 984; (g) M. Honda, S. Kuno, S. Sonehara, K.-i. Fujimoto, K. Suzuki, Y. Nakagawa and K. Tomishige, *ChemCatChem* 2011, **3**, 365; (h) J. Lv, Y. Shen, L. Peng, X. Guo and W. Ding, *Chem. Commun.* 2010, **46**, 5909; (i) M. Tamura, K. Sawabe, K. Tomishige, A. Satsuma and K.-i. Shimizu, *ACS Catal.* 2015, **5**, 20.
- 16 M. Wang, F. Wang, J. P. Ma, M. R. Li, Z. Zhang, Y. H. Wang, X. C. Zhang and J. Xu, *Chem. Commun.* 2014, **50**, 292.
- 17 M. I. Zaki, M. A. Hasan and L. Pasupulety, *Langmuir* 2001, **17**, 768.
- 18 Currently we have found some indentified substances after washing the used ceria. Much more future works are required.
- 19 H.-X. Mai, L.-D. Sun, Y.-W. Zhang, R. Si, W. Feng, H.-P. Zhang, H.-C. Liu and C.-H. Yan, *J. Phys. Chem. B* 2005, **109**, 24380.
- 20 T. X. T. Sayle, S. C. Parker and C. R. A. Catlow, *J. Chem. Soc., Chem. Commun.* 1992, 977.
- 21 M. Nolan, S. C. Parker and G. W. Watson, *Surf. Sci.* 2005, **595**, 223.
- 22 J. Z. Shyu, W. H. Weber and H. S. Gandhi, *J. Phys. Chem.* 1988, **92**, 4964.
- 23 (a) Z. Y. Pu, J. Q. Lu, M. F. Luo and Y. L. Me, *J. Phys. Chem. C* 2007, **111**, 18695; (b) Z. V. Popovic, Z. Dohcevic-Mitrovic, M. J. Konstantinovic and M. Scepovic, *J. Raman Spectrosc.* 2007, **38**, 750.
- 24 L. Meng, A. P. Jia, J. Q. Lu, L. F. Luo, W. X. Huang and M. F. Luo, *J. Phys. Chem. C* 2011, **115**, 19789.
- 25 Istadi and N. A. S. Amin, *J. Mol. Catal. A: Chem.* 2006, **259**, 61.
- 26 (a) S. Bodoardo, F. Figueras and E. Garrone, *J. Catal.* 1994, **147**, 223; (b) R. Buzzoni, S. Bordiga, G. Ricchiardi, C. Lamberti, A. Zecchina and G. Bellussi, *Langmuir* 1996, **12**, 930.
- 27 (a) H. Hattori, *Chem. Rev.* 1995, **95**, 537; (b) M. J. Climent, A. Corma, S. Iborra and J. Primo, *J. Catal.* 1995, **151**, 60; (c) Y. Zhu, S. Jaenicke and G. K. Chuah, *J. Catal.* 2003, **218**, 396.
- 28 K. Deori, C. Kalita and S. Deka, *J. Mater. Chem. A* 2015, **3**, 6909.

Graphical Abstract

